Int. J. Heat Mass Transfer. Vol. 29, No. 8, pp. 1159–1167, 1986
Printed in Great Britain

0017–9310/86 $3.00 + 0.00
Pergamon Journals Ltd.

Recent film boiling calculations: implication on fuel–coolant interactions

B. J. KIM and M. L. CORRADINI
University of Wisconsin—Madison, Madison, WI 53706, U.S.A.

Abstract—A transient film boiling model was developed to study the film boiling dynamics that would occur when a molten, spherical fuel droplet is immersed in a coolant. The focus of this study was to investigate the effects of noncondensable gas, coolant temperature and ambient pressure on film boiling during the initial growth phase. These parameters were found to have the greatest influence on the triggering of the small scale fuel–coolant interactions. The results indicate that the film generally stabilizes with more noncondensable gas present and higher coolant temperatures. Our calculations indicate that small ambient pressurizations cause violent fluctuation of the film pressure while higher ambient pressures suppress these oscillations. These results are in good agreement with Nelson's experimental data for a single fuel droplet in water.

1. INTRODUCTION

FOR AN energetic fuel–coolant interaction (FCI) to occur, film boiling between the fuel and coolant is a prerequisite for a coarse fuel–coolant mixture to develop. Only when there is an insulating vapor film is there enough time to mix the hot and cold components without premature rapid heat transfer taking place. Only a few analytical studies have been done to simulate transient vapor film boiling around a hot sphere [1, 2]. However, calculations were done up to only 1 ms, which was too short a time to describe even the initial growth behavior of film; usually it takes longer for the vapor film to grow and enter a quasi-steady state. The purpose of this study is to develop a dynamic model of film growth which can give the initial conditions for the film collapse phase which triggers the FCI; this is usually initiated by an external pressure pulse in the small scale, single droplet experiments [3, 4]. This dynamic model indicates interesting trends in the transient behavior of the vapor film before film collapse is induced and the explosion begins.

2. FORMULATION OF THE MODEL

Our model is of a spherical fuel droplet immersed in a large volume of coolant, Fig. 1, which is the characteristic of small scale, single droplet experiments. Our basic assumptions are:

1. The fuel–coolant system is spherically symmetric; it implies that the variation of the film thickness is small compared to droplet radius and is observed in the small scale FCI experiments [3, 4] that were analyzed.
2. All the vapor produced is retained in the film; no vapor generated was detached from the film during the initial film boiling in the experiments because of the small droplet radius and the large water subcooling.
3. The pressure in the film is spatially uniform; the film around the droplet is very thin and the time elapsing as a pressure disturbance is transmitted across the film is much less than the time involved in appreciable change in the average film pressure.
4. The vapor and other gases, if any, in the film are considered to be perfect gases; the critical point of the coolant is not approached during the film growth.
5. A small gaseous film initially exists at the surface of the sphere; the initial gaseous film is comprised of both the gas generated at the surface of the drop due to chemical reaction and the gas swept into the coolant as the droplet falls freely through the surrounding gas upon entering the water pool. In the model, only the gas swept into the coolant is considered.
6. Coolant and fuel liquid are considered to be incompressible; the velocity of the film–coolant interface is far less than the speed of sound.
7. The thermophysical properties are considered to be constant except the latent heat of the coolant and density of air; since the film undergoes severe oscillations during growth, the latent heat of coolant is given as a function of the saturation temperature of the coolant.

Mathematical formulations

The dynamic film boiling process was modelled by writing a momentum equation for film dynamics and an energy equation for each region of the system (fuel, coolant vapor and liquid) and linking each region by the appropriate boundary conditions. The integral approach was used in each region for the energy equations where the differential equation was integrated

NOMENCLATURE

a	acceleration
C_p	specific heat
G	gas constant
h	heat transfer coefficient
h_{fg}	latent heat of vaporization
k	thermal conductivity
M	molecular weight
P	pressure
R	droplet radius
R_δ	film radius
r	radius
T	temperature
t	time
U	velocity
V	volume.

Greek symbols

α	thermal diffusivity
β	accommodation coefficient
γ	gas index
δ	film thickness
ε	emissivity
θ	surface tension
λ	boundary-layer thickness
μ	viscosity
ρ	density
σ	Boltzmann constant.

Subscripts

c	coolant
ci	coolant bulk
co	coolant surface
f	film
g	gas
h	molten droplet
hi	droplet center
ho	droplet surface vs vapor surface at film–coolant interface
v	vapor

over the region and a temperature profile was assumed.

The momentum equation for film growth is modelled by a general Rayleigh equation [5], where the effect of viscosity and surface tension are included

$$\frac{dU}{dt} = \frac{1}{R_\delta} \times \left[\frac{P_f - P_\infty - (2\theta_c/R_\delta) - (4\mu_c/R_\delta)U}{\rho_c} - \frac{3}{2}U^2 \right]. \quad (1)$$

The evaporation or condensation rate is obtained from a simple kinetic theory of gas model under a nonequilibrium condition at the vapor–liquid interface [6]

$$\frac{dM_v}{dt} = 4\pi R_\delta^2 \beta \frac{M}{2\pi G}\left(\frac{P_{co}}{\sqrt{T_{co}}} - \frac{P_v}{\sqrt{T_{vs}}}\right) \quad (2)$$

where the accommodation coefficient was assumed to be 0.04 in this application; separate studies indicate that the effects of accommodation coefficient are negligible.

The velocity of the vapor–liquid interface is then given by

$$\frac{dR_\delta}{dt} = U + \frac{dM_v/dt}{4\pi R_\delta^2 \rho_c}. \quad (3)$$

The heat transfer in the fuel droplet is governed by Fourier's conduction equation

$$\frac{\alpha_h}{r^2}\frac{\partial}{\partial r}\left[r^2 \frac{\partial}{\partial r} T_h(r,t)\right] = \frac{\partial}{\partial t} T_h(r,t). \quad (4)$$

Since the temperature wave may not have penetrated to the center of droplet during the time of interest, the droplet is treated as a semi-infinite mass and integrated from $r = R - \lambda_h$ to $r = R$

$$\alpha_h \int_{R-\lambda_h(t)}^{R} d\left[r^2 \frac{\partial}{\partial r} T_h(r,t)\right] = \int_{R-\lambda_h(t)}^{R} \frac{\partial}{\partial t} T_h(r,t)\, dr. \quad (5)$$

A quadratic temperature profile satisfying the boundary conditions within the thermally active region is assumed as

$$T_h(r,t) = T_{hi} + (T_{ho} - T_{hi})\left(1 - \frac{R-r}{\lambda_h}\right)^2 \quad (6)$$

where the boundary conditions satisfied are

$$T_h(R-\lambda_h, t) = T_{hi}(t) \quad (7a)$$

$$T_h(R,t) = T_{ho}(t) \quad (7b)$$

$$\frac{\partial T_h(r,t)}{\partial r} = 0; \quad r = R - \lambda_h(t). \quad (7c)$$

When this temperature profile is substituted into equation (5), the result is

$$\left[\frac{1}{6} - \frac{1}{6}\left(\frac{\lambda_h}{R}\right) + \frac{1}{20}\left(\frac{\lambda_h}{R}\right)^2\right]\frac{d\lambda_h}{dt} = \frac{\alpha_h}{\lambda_h} + \frac{\lambda_h}{2(T_{hi} - T_{ho})} \times \left[\frac{1}{3} - \frac{1}{6}\left(\frac{\lambda_h}{R}\right) + \frac{1}{30}\left(\frac{\lambda_h}{R}\right)^2\right]\frac{dT_{ho}}{dt}. \quad (8)$$

The energy equation for the coolant is similar to equation (4) except that a radial convective term is included to account for the movement of the vapor

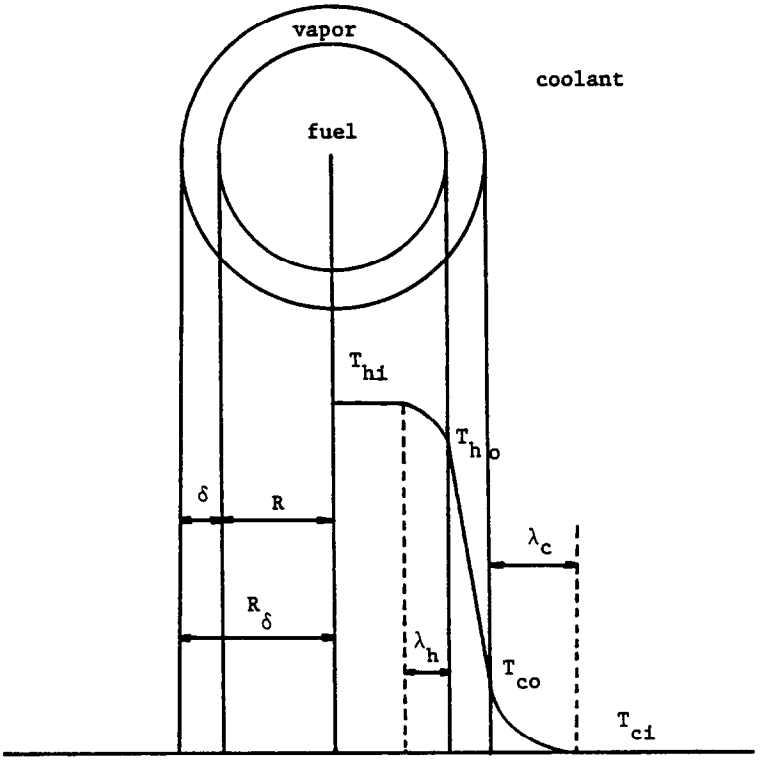

FIG. 1. Schematic diagram of dynamic film growth and collapse model.

film and the subsequent movement of the liquid

$$\frac{\partial T_c}{\partial t}+\frac{\partial r}{\partial}\cdot\frac{\partial T_c}{\partial r}=\frac{\alpha_c}{r^2}\left[\frac{\partial}{\partial r}\left(r^2\frac{\partial T_c}{\partial r}\right)\right]+K\cdot Q_r'' \quad (9)$$

where the last term on the RHS is the fraction of radiation energy deposited in the thermally active region of coolant. The radiation energy from the fuel was considered as volumetric energy generation within and without the thermal boundary layer. Constant K is given as a function of the surface temperature of droplet and the thickness of thermal boundary layer in the coolant. Again a parabolic temperature profile is assumed in the liquid thermal boundary layer. Boundary conditions are

$$T_c(R_\delta, t) = T_{co}(t) \quad (10a)$$

$$T_c(R_\delta+\lambda_c, t) = T_{ci}(t) \quad (10b)$$

$$\frac{\partial T_c(r,t)}{\partial r} = 0; \quad r = R_\delta+\lambda_c(t). \quad (10c)$$

The temperature profile in the thermally active region of coolant becomes

$$T_c(r,t) = T_{ci}+(T_{co}-T_{ci})\left(1-\frac{r-R_\delta}{\lambda_c}\right)^2. \quad (11)$$

By substituting this temperature profile into equation (9) and integrating over the thermal boundary layer, it becomes

$$\left[\frac{1}{6}+\frac{1}{6}\left(\frac{\lambda_c}{R_\delta}\right)+\frac{1}{20}\left(\frac{\lambda_c}{R_\delta}\right)^2\right]\frac{d\lambda_c}{dt}$$
$$=\frac{\alpha_c}{\lambda_c}+\frac{1}{2}U+\frac{KR^2\varepsilon\sigma T_{ho}^4}{2R_\delta^2\rho_c c_{pc}(T_{co}-T_{ci})}$$
$$-\frac{\lambda_c}{2(T_{co}-T_{ci})}\left[\frac{1}{3}+\frac{1}{6}\left(\frac{\lambda_c}{R_\delta}\right)+\frac{1}{30}\left(\frac{\lambda_c}{R_\delta}\right)^2\right]\frac{dT_{co}}{dt}$$
$$-\left[\frac{1}{2}+\frac{1}{3}\left(\frac{\lambda_c}{R_\delta}\right)+\frac{1}{12}\left(\frac{\lambda_c}{R_\delta}\right)^2\right]\frac{dR_\delta}{dt}. \quad (12)$$

Using a lumped parameter energy equation for the vapor film, the energy conservation equation is given as

$$\frac{d}{dt}[M_v u_v+M_g u_g] = Q_v-P_f\frac{dV}{dt}$$
$$+4\pi R_\delta^2\beta\sqrt{\frac{M}{2\pi G}}\left[\frac{P_{co}}{\sqrt{T_{co}}}h_v(T_{co},P_{co})\right.$$
$$\left.-\frac{P_v}{\sqrt{T_{vs}}}h_v(T_{vs},P_v)\right] \quad (13)$$

where

$$Q_v = 4\pi R_\delta^2\left[\frac{2k_v}{\delta}(T_v - T_{co}) - \frac{2k_c}{\lambda_c}(T_{co} - T_{ci})\right] \tag{14}$$

$$h_v(T_v, P_v) = C_{pv}(T_v - T_{co}) + h_{fg} + C_{pc}(T_{co} - T_{ci}) \tag{15}$$

u_v and h_v are the specific internal energy and specific enthalpy of vapor, respectively. As long as the lumped energy equation is used, the temperature profile assumed for the vapor film does not affect the general film behavior very much.

Another relation between the rate of change of T_{ho} and λ_h is obtained from the boundary condition at the droplet–vapor interface given as

$$\left[\frac{2k_h}{\lambda_h} + \frac{2k_v}{\delta} + 4\varepsilon\sigma T_{ho}^3\right]\frac{dT_{ho}}{dt} = -\frac{2k_h}{\lambda_h^2}(T_{hi} - T_{ho})\frac{d\lambda_h}{dt} + \frac{2k_v}{\delta^2}(T_{ho} - T_v)\frac{dR_\delta}{dt} + \frac{2k_v}{\delta}\frac{dT_v}{dt}. \tag{16}$$

The heat transfer rate in the coolant was determined by choosing the higher transfer rate between conduction and convection at the vapor–liquid interface. The forced convective heat transfer coefficient is calculated from the correlation for the flow past a solid sphere [7] and is given by

$$Nu = 2.0 + 0.6Re^{1/2}Pr^{1/3}. \tag{17}$$

The final equation is obtained from the vapor film–liquid coolant boundary condition given as

$$\left(\frac{2k_v}{\delta} + \frac{2k_c}{\lambda_c}\right)\frac{dT_{co}}{dt} = \frac{2k_v}{\delta}\frac{dT_v}{dt} - \frac{d}{dt}\left[h_{fg}\beta\sqrt{\frac{M}{2\pi G}}\left(\frac{P_{co}}{\sqrt{T_{co}}} - \frac{P_v}{\sqrt{T_{vs}}}\right)\right] + \frac{2k_v}{\delta^2}(T_v - T_{co})\frac{dR_\delta}{dt} + \frac{2k_c}{\lambda_c^2}(T_{co} - T_{ci})\frac{d\lambda_c}{dt}. \tag{18}$$

For a forced-convection-dominating heat transfer, the rate of change of λ_c is neglected and the conduction heat transfer coefficient in the coolant is replaced by the forced-convection heat transfer coefficient.

The pressure in the vapor film is determined from Dalton's law of partial pressure

$$P_f = P_v + P_g \tag{19}$$

where vapor is treated as an ideal gas and noncondensable gas is assumed to behave isentropically. The initial noncondensable gas film thickness is considered to be some fraction of the boundary-layer thickness of the flow over sphere before it enters the coolant pool and given as

$$\delta_g = C \cdot D \cdot (Re_D)^{-1/2} \tag{20}$$

where the constant C was parametrized and varied from 0.01 to 0.1 in this model.

Equations (1)–(3), (8), (12), (13), (16) and (18) constitute a set of nonlinear, first-order differential equations in the eight time-dependent variables R_δ, U, T_v, T_{co}, T_{ho}, λ_h, λ_c and M_v. A simultaneous solution has been obtained by using the one-step Runge–Kutta–Merson technique which is a modification of fourth-order Runge–Kutta integration [8].

3. APPLICATIONS OF THE MODEL: RESULTS AND DISCUSSIONS

The model developed has been applied to the growth of a vapor film around a molten iron oxide droplet in water; this fuel–coolant pair was used by Nelson [3, 4] in his single droplet FCI experiments. The initial conditions for the base case experiments are given in Table 1. Initially the rapid vaporization results in a pressure rise in the film which accelerates the film–coolant interface outward. However, the outward motion of the interface continues beyond the equilibrium position. Thus the film pressure falls below the ambient pressure leading to deceleration of the interface. The movement of the film–coolant interface is reversed and the film starts to collapse. This cycle of growth and partial collapse repeats with an increase in the film thickness and the amplitude of the film pressure oscillations until it reaches its maximum values. Then the film oscillation amplitude eventually decreases, and appears to enter a stable state. This stable state occurs when the film thickness reaches a quasi-steady-state value and the heat transfer rate across the film equals the heat transfer into the liquid water [e.g. see Figs. 2(a) and (2b)]. Under certain sets of initial conditions (i.e. fuel and coolant temperature, ambient pressure, noncondensable gas film thickness) we have observed that the film oscillations do not die away but continue for long periods of times at large amplitude. We have verified that these prolonged oscillations are not numerically based. Therefore, it appears that they represent the case where the film is not inherently stable and surface instabilities (e.g. Taylor instabilities) would cause fuel–coolant contact and local film collapse. This occurs when the film pressure oscillations become large enough to induce the coolant vapor–liquid interface to become unstable. For example, if the film pressure increases significantly above ambient pressure conditions, there is an acceleration from the less

Table 1. Initial condition values used in these calculations

Droplet composition	iron oxide ($FeO_{1.3}$)
Droplet radius	1.4 mm
Initial droplet temperature	2233 K
Coolant composition	water
Coolant bulk temperature	300 K
Ambient pressure	0.1 MPa

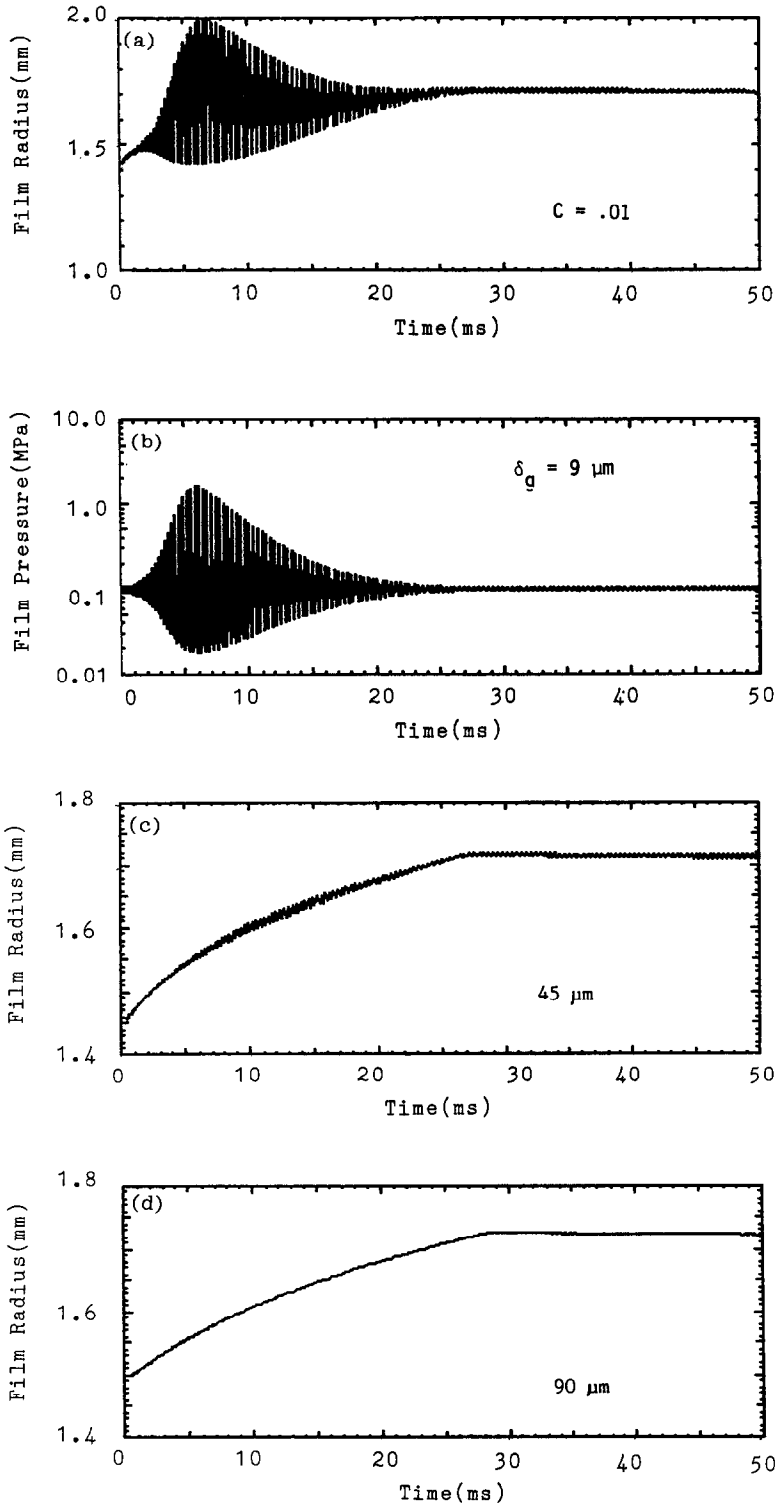

FIG. 2. (a,b) Vapor film radius and pressure as a function of time during film growth. (c,d) Effect of initial gas film thickness on vapor film radius–time history during film growth.

dense vapor to the more dense liquid coolant and Taylor instabilities would form at the interface. As the pressure becomes larger the wave number for these instabilities become larger (wavelength smaller) and their growth rate increases. Based on Taylor linear theory the fastest growing wavelength is given by

$$\lambda_m = 2\pi\sqrt{\frac{3\theta}{\Delta\rho a}} \tag{21}$$

where the acceleration, a, is derived from the film pressure difference, ΔP, as

$$a = \frac{\Delta P}{\rho_f R_\delta}. \tag{22}$$

For example, using conditions in Table 1, the pressure difference required to impose a wavenumber of 20 on the vapor–liquid interface around the fuel drop (i.e. 20 unstable waves around the circumference) would be a ΔP of 0.1 MPa. This type of pressure difference can occur in certain situations.

Given this instability growth the FCI could be triggered by the local film collapse. This set of initial conditions is of importance to us because they probably represent the conditions where Nelson found the single fuel droplet tests to be easily triggered shortly after entering the water pool. Therefore, we have parametrically investigated the set of initial conditions which Nelson found to be important in affecting the triggering of the FCI in the single droplet tests (i.e. gas entrained, coolant temperature and ambient pressure). We feel one can explain the change in triggerability due to the film growth dynamics when these initial conditions are varied.

Effect of initial noncondensable gas film thickness

The influence of the initial noncondensable gas on the film growth is significant (Fig. 2). The oscillations of film were diminished enormously with an increase of the initial noncondensable gas film thickness due to its retardation of the initial heat transfer across the film and its damping effect on pressure fluctuation. Figures 2(c) and (d) suggest that as the amount of noncondensable gas is increased the initial heat transfer rate decreases proportionally. This decreases the rate of growth of the film and film overexpansion and subsequent oscillations are eliminated. In Figs. 2(c) and (d) the initial gas film thickness was increased by a factor of 5 and 10 from that in Figs. 2(a) and (b), respectively. This result suggests that the occurrence of spontaneous triggering of the single droplet FCI at a lower drop fall height can be explained by a smaller amount of noncondensable gas; i.e. the lower drop fall height reduces the entry Reynolds number and therefore the amount of noncondensable gas entrained in the film causing large film and pressure oscillations, film collapse and FCI triggering.

Effect of coolant temperature

Figure 3 shows that the decreasing water subcooling stabilizes film boiling, which is consistent with experimental data [9]. Damped oscillations at lower sub-

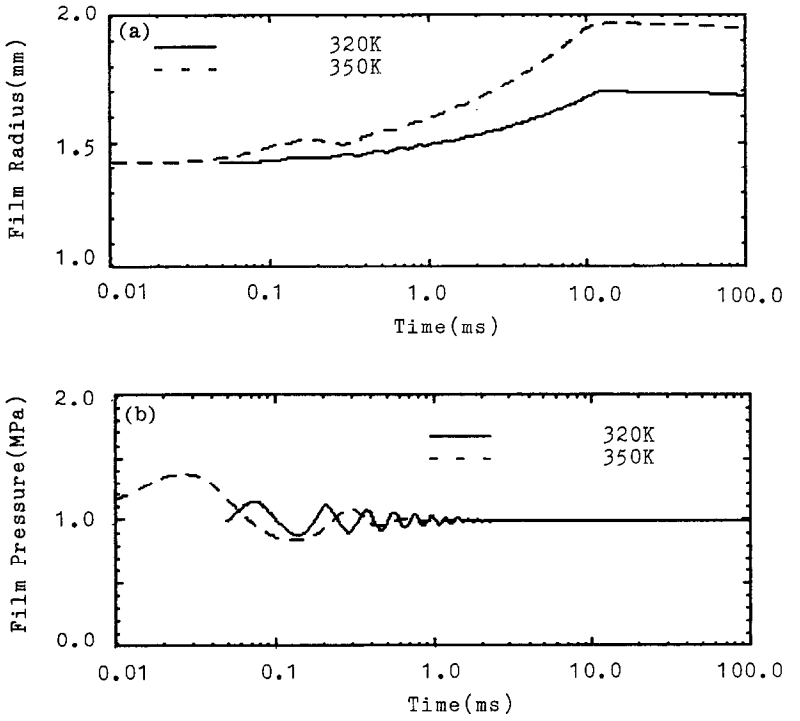

FIG. 3. Effect of water temperature on vapor film growth (constant ambient pressure). (a) Vapor film radius–time history. (b) Vapor film pressure–time history.

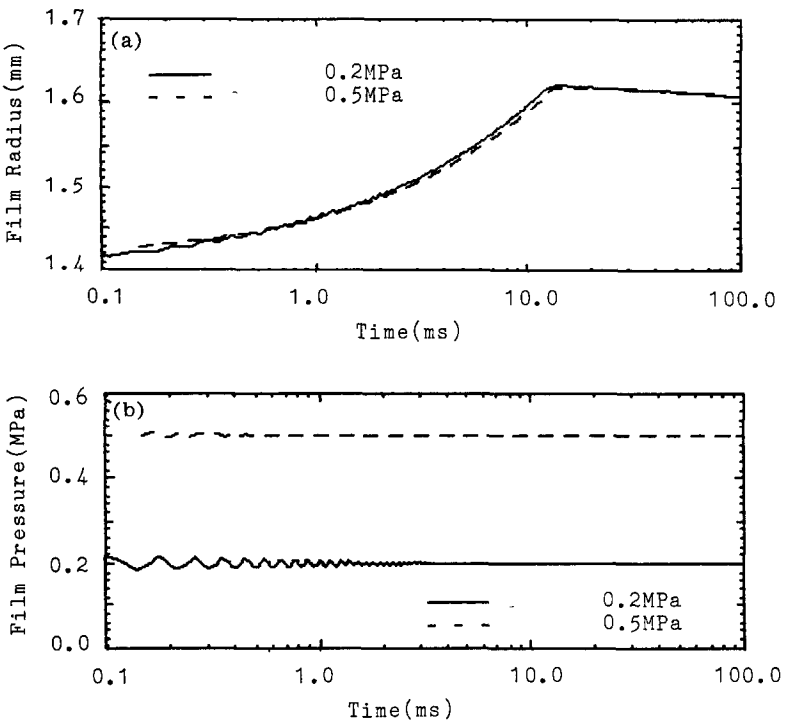

FIG. 4. Effect of water temperature on vapor film pressure-time history during film growth (constant water subcooling).

cooling are due to the continuous and higher evaporation rate which tends to prevent the pressure in the film falling below the ambient pressure. Thus lower water subcooling makes film collapse more difficult due to these effects on forming a more stable and thicker vapor film around the drop.

At constant water subcooling, the oscillations of the pressure in the film have a smaller amplitude and damp more quickly with higher ambient pressure (Fig. 4). Higher ambient pressure suppresses the oscillation of the film and higher water temperature induces easier vaporization leading to the more stable film. These effects are synergetic and stabilize the film almost from its first growth stages.

Effect of ambient pressure

The duration of film pressure fluctuation becomes shorter as ambient pressure increases as illustrated in Fig. 5. Also the time required to reach its maximum film pressure during the film growth also decreases with ambient pressure. The maximum film pressure increases sharply as the ambient pressure increases from 0.1 to 0.2 MPa and then remains almost unchanged as P_∞ increases up to 0.4 MPa. For further increases in ambient pressure, the peak film pressure generated decreases relatively slowly. In some aspects this film behavior explains why small ambient pressurizations lead to the easier initiation of FCI and shorter interaction time. These effects of ambient pressure are related to the suppression of oscillation and easier vaporization due to the lower latent heat of vaporization of water at higher ambient pressure against the higher subcooling of water.

4. CONCLUSIONS AND RECOMMENDATIONS

Our conclusion is that a simple model of film boiling dynamics can qualitatively predict the characteristics of small scale, single droplet film dynamics in terms of film growth and thickness, film pressure oscillation and amplitude, and time scale—which are strong functions of evaporation rate throughout the boiling process. The initial noncondensable gas film thickness and coolant temperature have consistent and predictable effects on film growth by diminishing the oscillation of film pressure. Ambient pressure affects film behavior depending upon the magnitude of pressurization, and results in the most violent pressure oscillation at a certain intermediate ambient pressure. However, the influence of any one parameter on the film boiling can be suppressed or enhanced by varying another parameter; they are closely interrelated to each other.

Once the initial conditions for the collapse phase are obtained, film collapse behavior due to external pressure pulse can be examined. During this phase, film pressure is considered to increase rapidly and closer liquid–liquid contact due to the surface instabilities is very likely. Therefore we are continuing to study film collapse behavior in connection with surface instabilities and local fuel–coolant contact.

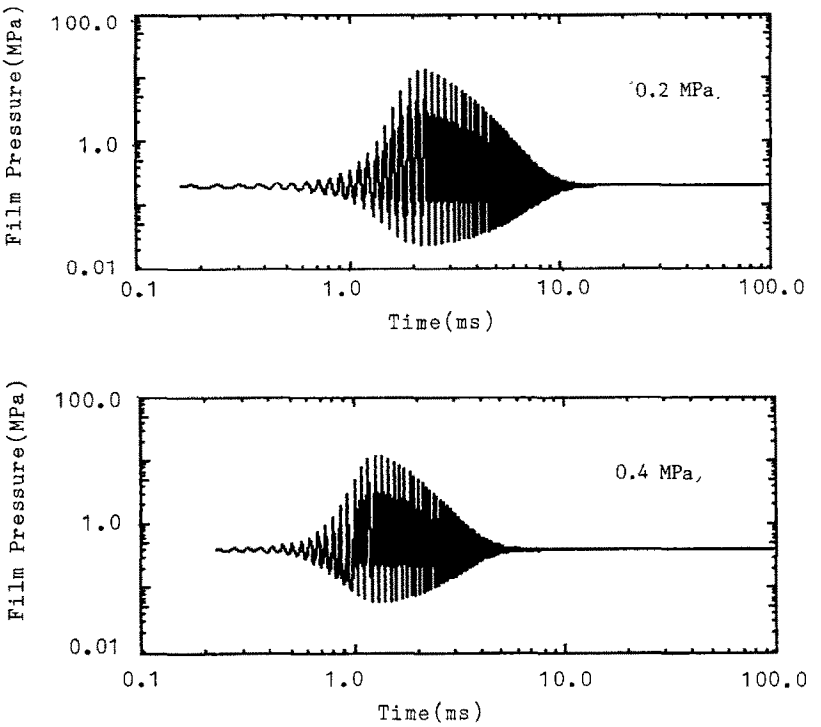

FIG. 5. Effect of ambient pressure on vapor film pressure–time history during film growth.

REFERENCES

1. M. S. Kazimi, Theoretical studies of some aspects of molten fuel–coolant interactions. Ph.D. thesis, MIT, Cambridge, MA (May 1973).
2. M. L. Corradini, Phenomenological modelling of the triggering phase of small-scale steam explosion experiments, *Nucl. Sci. Engng* **78**, 151–170 (1981).
3. L. S. Nelson and P. M. Duda, Steam explosion experiments with single drops of iron oxide melted with CO_2 laser, Sandia Laboratories, SAND81-1346, NUREG/CR-2295 (September 1981).
4. L. S. Nelson and P. S. Duda, Steam explosion experiments with single drops of iron oxide melted with a CO_2 laser; Part 2. Parametric studies, Sandia Laboratories, SAND82-1105, NUREG/CR-2718 (1982).
5. Lord Rayleigh, On the pressure developed in a liquid during the collapse of a spherical cavity, *Phil. Mag.* **94** (1917).
6. R. W. Schrage, *A Theoretical Study of Interphase Mass Transfer*. Columbia University Press, New York (1953).
7. W. H. McAdams, *Heat Transmission*, 3rd edn. McGraw-Hill, New York (1954).
8. G. N. Lance, *Numerical Methods for High Speed Computer*, pp. 54–57. Iliffe, London (1960).
9. S. J. Board, An experimental study of energy transfer process relevant to thermal explosion, *Int. J. Heat Mass Transfer* **14**, 1631–1641 (1971).

NOUVEAUX CALCULS D'EBULLITION EN FILM: INTERACTIONS ENTRE COMBUSTIBLE ET REFRIGERANT

Résumé—Un modèle d'ébullition en film est développé pour étudier la dynamique de l'ébullition en film qui se produit lorsqu'une gouttelette de combustible sphérique est entourée d'un réfrigérant. Le point central de l'étude est de dégager l'effet de gaz incondensable, de la température du réfrigérant et de la pression ambiante sur l'ébullition pendant la phase initiale. Les résultats montrent que généralement le film se stabilise quand augmentent la présence d'incondensable et la température du réfrigérant. D'après les calculs, une faible pressurisation de l'ambiance cause une fluctuation violente sur la pression du film, tandis que des pressions ambiantes plus élevées suppriment ces oscillations. Ces résultats sont en bon accord avec les données expérimentales de Nelson pour une gouttelette de combustible dans l'eau.

NEUE BERECHNUNGEN ZUM FILMSIEDEN: ANWENDUNG AUF BRENNSTOFF–KÜHLMITTEL WECHSELWIRKUNGEN

Zusammenfassung—Ein instationäres Filmsiedemodell wurde entwickelt, um die Dynamik des Filmsiedens zu untersuchen, die auftreten würde, wenn ein geschmolzener kugelförmiger Brennstofftropfen in ein Kühlmittel fällt. Das Ziel dieser Studie war es, die Einflüsse von nicht kondensierbaren Gasen, Kühlmitteltemperatur und Umgebungsdruck während der anfänglichen Wachstumsphase zu untersuchen. Es stellte sich heraus, daß diese Parameter den größten Einfluß auf den Auslösemechanismus der Brennstoff–Kühlmittel Wechselwirkungen im Kleinen haben. Die Ergebnisse zeigen, daß sich der Film grundsätzlich bei Anwesenheit von mehr nichtkondensierbarem Gas und bei höheren Kühlmitteltemperaturen stabilisiert. Unsere Berechnungen zeigen, daß kleine Umgebungsdrücke starke Schwankungen des Filmdruckes verursachen, während höhere Umgebungsdrücke diese Schwingungen unterdrücken. Diese Ergebnisse stimmen gut mit den experimentellen Daten von Nelson für einen Brennstofftropfen in Wasser überein.

НОВЫЕ РАСЧЕТЫ ПЛЕНОЧНОГО КИПЕНИЯ: ПРИМЕНЕНИЕ К ВЗАИМОДЕЙСТВИЯМ ТОПЛИВО–ОХЛАДИТЕЛЬ

Аннотация—Модель переходного пленочного кипения разработана для изучения динамики пленочного кипения, имеющего место в случаях, когда расплавленная сферическая частица топлива погружена в охладитель. Цель работы—исследование влияния неконденсирующегося газа, температуры охладителя и давления окружающей среды на пленочное кипение в начальный период роста фазы. Найдено, что эти параметры оказывают наибольшее влияние на возникновение мелкомасштабных взаимодействий топливо–охладитель. Результаты показывают, что пленка в основном стабилизируется в присутствии неконденсирующегося газа и при больших температурах охладителя. Из расчетов видно, что небольшие повышения давления окружающей среды вызывают сильные флуктуации давления пленки, в то время как бóльшие давления окружающей среды подавляют эти колебания. Результаты хорошо согласуются с экспериментальными данными Нельсона для одиночной капли топлива в воде.